



**HAL**  
open science

## Size and chemical structure impact of lignin biopolymer over performances of next-generation sunscreens

Victor Girard, Hubert Chapuis, Nicolas Brosse, Nadia Canilho, Stéphane Parant, Laurent Marchal-Heussler, Isabelle Ziegler-Devin

### ► To cite this version:

Victor Girard, Hubert Chapuis, Nicolas Brosse, Nadia Canilho, Stéphane Parant, et al.. Size and chemical structure impact of lignin biopolymer over performances of next-generation sunscreens. 2024. hal-04503643

**HAL Id: hal-04503643**

**<https://hal.science/hal-04503643>**

Preprint submitted on 13 Mar 2024

**HAL** is a multi-disciplinary open access archive for the deposit and dissemination of scientific research documents, whether they are published or not. The documents may come from teaching and research institutions in France or abroad, or from public or private research centers.

L'archive ouverte pluridisciplinaire **HAL**, est destinée au dépôt et à la diffusion de documents scientifiques de niveau recherche, publiés ou non, émanant des établissements d'enseignement et de recherche français ou étrangers, des laboratoires publics ou privés.

1 Size and chemical structure impact of lignin  
2 biopolymer over performances of next-generation  
3 sunscreens.

4 *Victor Girard,<sup>†</sup> Hubert Chapuis,<sup>†</sup> Nicolas Brosse,<sup>†</sup> Nadia Canilho,<sup>‡</sup> Stéphane Parant,<sup>‡</sup> Laurent*  
5 *Marchal-Heussler,<sup>§</sup> Isabelle Ziegler-Devin<sup>†\*</sup>*

6 <sup>†</sup>LERMAB, Université de Lorraine, INRAe, GP4W F-54000 Nancy, France

7 <sup>‡</sup>L2CM, Université de Lorraine, CNRS, F-54000 Nancy, France

8 <sup>§</sup>ENSIC, Université de Lorraine, F-54000 Nancy, France

9

10 KEYWORDS : Lignin, Sunscreens, Lignin Nanoparticles, Organosolv, UV-shielding, Eco-  
11 friendly production

12

13

14

15

16

17

18 ABSTRACT

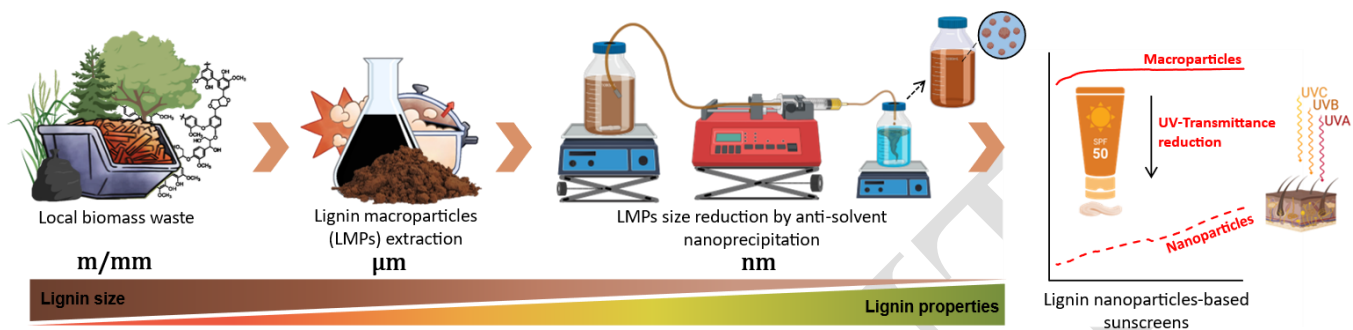
19 In recent years, growing concerns about the harmful effects of synthetic UV filters on both humans  
20 and the environment raised awareness about natural sun blockers. Lignin, considerate as the most  
21 abundant aromatic renewable polymer on earth, emerges as a strong contender for the development  
22 of next-generation sunscreens due to its inherent UV ray's absorbance properties, as well as its  
23 distinctive qualities as a green, biodegradable, and biocompatible material. Furthermore, lignin  
24 current limitations such as dark color and poor dispersity can potentially be overcome with particle  
25 size reduction to nano scale, paving the way for improved UV protection and enhanced  
26 formulation. In this study, 100 – 200 nm lignin nanoparticles (LNPs) were eco-friendly prepared  
27 from various biomass waste with anti-solvent precipitation method using water and ethanol.  
28 Initially, pure lignin macroparticles (LMPs) were extracted from beech, spruce and wheat using  
29 ethanol-Organosolv treatment (OL) in opposition to sulfur-rich kraft lignin (KL). We prepared  
30 sunscreen lotions from these LMPs and LNPs at different concentrations (1, 5 and 10 wt%)  
31 showing distinct UV-shielding properties depending on biomass type and particles size. Indeed,  
32 our results showed that for same lignin, transition from macro to nano scale multiplied sunscreens  
33 sun protection factor (SPF) and efficacy between 2.5 and 6. As an example for wheat straw, SPF  
34 was improved from 7.5 to 42 for same LMPs and LNPs 5 wt%, generating high quality green  
35 sunscreens. This study confirms that lignin polymer, often erroneously regarded as waste, can  
36 significantly contribute to the development of green and innovative valorizations in alignment with  
37 the principles of green chemistry.

38

39

40 GRAPHICAL ABSTRACT

41



42

43

44

45

46

47

48

49

50

51

52

53

PREPRINT

## 54 INTRODUCTION

55 In a world where the growing concerns of environmental sustainability and improved ultraviolet  
56 (UV) radiation levels caused by ozone layer depletion due to human activity converge, the  
57 development of sunscreens that are both effective in shielding against harmful UV radiation and  
58 eco-friendly has become an increasingly pressing challenge.

59 Sunburn, skin damage or potential development of cancer can be attributed to prolonged UVB  
60 (280-320 nm) exposure compare to less energetic UVA (320-400 nm).<sup>1,2</sup> In response to these  
61 concerns, traditional commercial sunscreens have relied on contentious organic and inorganic UV  
62 filters,<sup>3</sup> such as titanium dioxide (TiO<sub>2</sub>)<sup>4</sup> to protect human skin from UV rays, despite the  
63 significant apprehensions including high environmental impact and persistence,<sup>5</sup> skin sensitivities  
64 and limited UV protection spectrum.<sup>6</sup> As an example, it has been recently proved that common  
65 chemical or physical UV absorbers like ZnO, TiO<sub>2</sub>, oxybenzone, octocrylene or octinoxate were  
66 responsible of marine ecosystems modification<sup>7</sup> and coral bleaching<sup>8,9</sup>. This prompted Australia  
67 and Hawaii<sup>7,10</sup> to prohibit these UV-active components regarding the annual 14,000 tons<sup>11</sup> of  
68 sunscreen that end up in world's oceans.<sup>12</sup>

69 In this context, lignin, the most abundant aromatic biopolymer<sup>13-16</sup> constituting 30% of the  
70 nonfossil organic carbon in nature<sup>17,18</sup> with proved high UV absorption<sup>19-31</sup> and low cytotoxicity<sup>32-  
71 37</sup>, presents tremendous potential for next-generation sunscreens. Lignin complex polymer  
72 structure contains phenylpropane units composed of guaiacyl (G), syringyl (S) and p-  
73 hydroxyphenyl (H) monomeric units linked by aryl ether and carbon-carbon bonds (**Figure 1**).<sup>38,39</sup>  
74 Furthermore, lignin UV-absorbing properties are related to functional groups such as phenolic,  
75 methoxyl groups, ketone, intramolecular hydrogen bond and other chromophores<sup>40-42</sup> making this

76 sustainable polymer an excellent absorber in UVB-UVA wavelength area targeted by wide-range  
77 of sunscreens.<sup>12</sup>

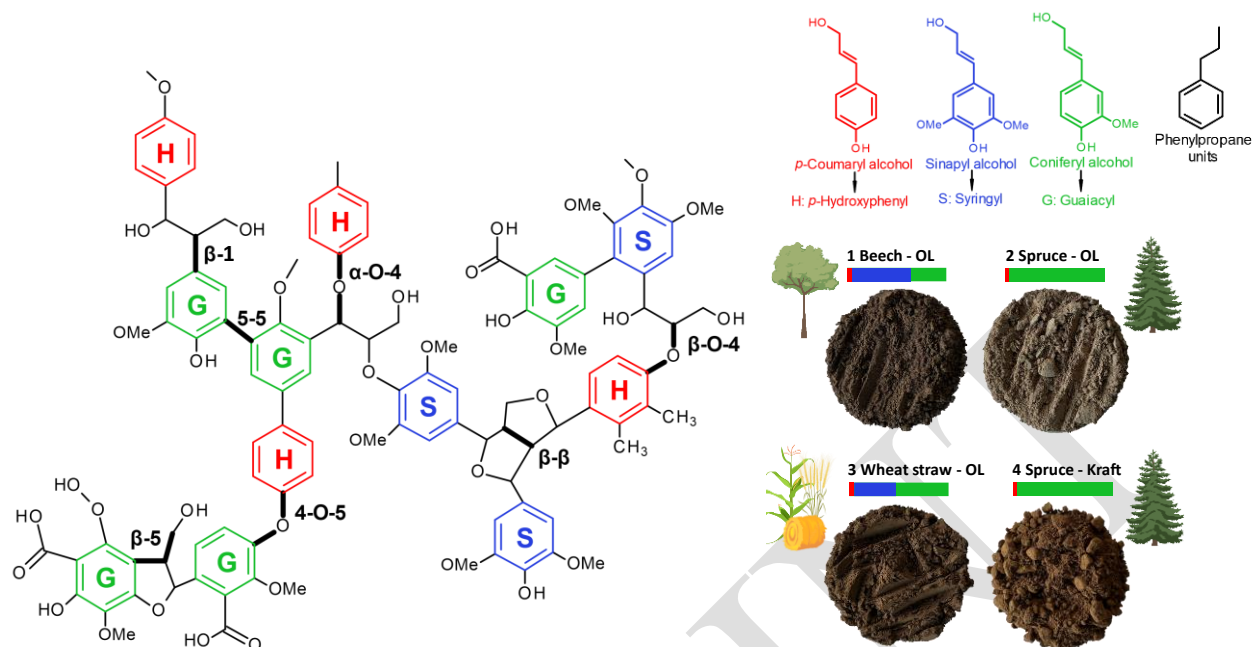
78 Despite great potential, the annually 50 million tons of generated lignin are still basically used as  
79 an energy source<sup>43-45</sup> because of processing challenges,<sup>46</sup> inherent heterogeneity of the  
80 macromolecular structure depending of isolation methods and biomass nature,<sup>47</sup> as well as too  
81 large particles limiting industrial applications. For now, lignin studies and valuations were mainly  
82 focused on technical lignins<sup>48</sup> like liginosulfonate or kraft lignin regardless of environmental  
83 limitations<sup>49,50</sup> and presence of sulfur,<sup>17,51</sup> which immediately hinders many possible uses like in  
84 cosmetics.<sup>52</sup>

85 However, lignin biopolymer could take benefits of both, novel eco-friendly isolation process like  
86 organosolv alongside the emerging integration of nanotechnology in cosmetics to address current  
87 limitations. Precisely, the extensive reach of nanotechnology in the cosmetic industry, as seen with  
88 ZnO and TiO<sub>2</sub> inorganic UV filters, results from enhanced properties of nanoparticles including  
89 size, stability, shape, reactivity, color or solubility.<sup>53</sup> Recent studies showed that lignin inherent  
90 heterogeneity, dark color, poor dispersibility can be overcome from particle size reduction,<sup>26</sup> while  
91 maintaining size over 100 nm to avoid skin absorption risks. For example, Qian et al.<sup>22</sup> showed  
92 that sun protection factor (SPF) of mixed sunscreens with lignin is boosted according to particle  
93 size reduction attesting the improved properties.

94 Various methods, such as nano-precipitation,<sup>54-60</sup> mechanical and ultrasound treatments,<sup>61-65</sup> or  
95 aerosol processing,<sup>66</sup> have been investigated for producing lignin nanoparticles (LNPs) with linked  
96 properties (size, shape, stability and reactivity).<sup>67</sup> Unfortunately, most of precedent listed studies  
97 used KL, rarely referred biomass source but also LNPs yields and real impact of particle size

98 reduction over UV-absorbing properties which still give incomplete view on lignin value for next-  
99 generation sunscreens.

100 Knowing that organosolv isolation process produced higher UV-shielding lignin's compare to  
101 others extraction methods as demonstrated by Qian et al.<sup>20</sup> and Tan et al.<sup>68</sup>, in our study we  
102 performed a global sustainable method from various biomass waste for pure lignin extraction (OL)  
103 and particles size reduction (nano-precipitation). Using this process, were able to generate  
104 concentrated suspensions of LNPs with improved characteristics and size around 150 nm while  
105 having high production yields. Then, we developed LMPs and LNPs based-sunscreens to highlight  
106 size reduction interest in UV-absorbing properties regarding pure cream and sunscreen. As lignin  
107 UV-absorbing properties are related to chemical structure (analyzed by SEC and NMR HSQC and  
108 <sup>31</sup>P), which varies according to the feedstock type, we evaluated the prepared sunscreens with  
109 different input (hardwood, softwood, grasses) and lignin type (KL, OL) to determine the most  
110 suitable lignin chemical structure for UV-absorption. Lignin based-sunscreens comparisons with  
111 commercial SPF 10 and SPF 30 sunscreens containing nano TiO<sub>2</sub> were also made as relevant result  
112 for a potential industrial integration.



113  
 114 **Figure 1.** Lignin chemical structure with the main linkages and the proportion of the different  
 115 monolignols G, S and H according to biomass type. Photographs of the organosolv extracted  
 116 lignin's with beech (1), spruce (2) and wheat straw (3). Comparison with kraft lignin from spruce  
 117 (4).

## 118 MATERIALS AND METHODS

119 **Raw materials.** Commercial kraft lignin was provided from the Lineo™ Prime W by Stora Enso  
 120 process (CAS Number 8068-05-1). Organosolv (OL) lignin was extracted from three distinct and  
 121 local waste biomass from Vosges forests and meadows (Grand Est Region, France). Selected waste  
 122 included beech (*Fagus Sylvatica*), spruce (*Picea Abies* L.) and wheat straw (*Triticum*) provided  
 123 from the French National School of Wood Technologies and Timber Engineering (ENSTIB  
 124 Épinal, France) and the "Bergerie de Straiture" sheepfold (Ban-Sur-Meurthe-Clefcy, France). Pure  
 125 cream used was NIVEA® Soft moisturizing skin care cream (200 ml) (Art.-No. 89050). Sunscreen

126 lotions were GARNIER® Latte protettivo SPF 10 (200 ml) and CIEN® Sun SPF 30 (75 ml). Cream  
127 and Sunscreen lotions were purchased from European drug markets.

128 **Biomass chemical characterization.** Chemical composition analysis, following National  
129 Renewable Energy Laboratory (NREL) labelled protocols and TAPPI method T222, was  
130 conducted on biomass powder. The procedure involved ash content determination (NREL/TP-510-  
131 42622), Soxhlet extraction (NREL/TP-510-42619), and analysis of acid insoluble lignin and  
132 monomeric sugar contents from free extractive biomass (NREL /TP-510-42618 and TP-510-  
133 42623). High-Performance Anion Exchange Chromatography coupled with Pulsed Amperometry  
134 Detection (HPAE-PAD, ICS-3000 Dionex®) was employed for monomeric sugar analysis  
135 (CarboPac PA-20 Dionex® analytical column). The composition gradient involved ultrapure water  
136 and NaOH solutions. Fucose, arabinose, rhamnose, galactose, glucose, xylose, mannose,  
137 galacturonic acid, and glucuronic acid were determined via external calibration (Sigma-Aldrich).  
138 Chemical content were (1) Beech: extractives =  $2.67 \pm 0.27$  (%w/w), cellulose =  $47.80 \pm 1.47$   
139 (%w/w), hemicelluloses =  $22.52 \pm 0.86$  (%w/w), lignin =  $23.70 \pm 0.25$  (%w/w) and ashes  $0.73 \pm$   
140  $0.01$  (%w/w) (2) Spruce: extractives =  $2.14 \pm 0.24$  (%w/w), cellulose =  $45.06 \pm 1.19$  (%w/w),  
141 hemicelluloses =  $21.41 \pm 1.19$  (%w/w), lignin =  $27.86 \pm 0.33$  (%w/w) and ashes  $0.36 \pm 0.01$   
142 (%w/w) (3) Wheat straw: extractives =  $0.56 \pm 0.15$  (%w/w), cellulose =  $49.56 \pm 1.05$  (%w/w),  
143 hemicelluloses =  $23.21 \pm 0.69$  (%w/w), lignin =  $20.52 \pm 0.24$  (%w/w) and ashes  $6.34 \pm 0.07$   
144 (%w/w).

145 **Lignin Macroparticles (LMPs) extraction.** Macroscale lignin from local biomass was obtained  
146 by employing eco-friendly OL treatment. For this purpose, biomass waste was first coarsely  
147 crushed with Retsch® cross beater mill SK100 into  $\varnothing 8$  mm particles prior to OL extraction process.  
148 In a PARR® 4568 pressurized 2-liter bench top reactor, 100 g of dry biomass underwent 1 h

149 treatment at 200 °C in a 60/40 v/v EtOH/H<sub>2</sub>O solution maintaining a liquid/solid ratio of 10/1. The  
150 reactor was then quickly cooled in an ice bath to stop the chemical reaction. Extracted black liquor  
151 was separated from solid phase through vacuum filtration. The lignin contained in black liquor  
152 mixture was isolated by direct precipitation with cold distilled water at a 1/3 v/v ratio. After 1 h,  
153 the precipitated lignin was filtered via vacuum filtration using a 1.6 µm glass macrofibres filter.  
154 Finally, the separated lignin was washed with 500 mL of distilled water before drying in a  
155 controlled oven at 40 °C for 2 days. LMPs powders were stored in a dark room before further  
156 analysis. For milled wood lignin (MWL) extraction, the method is based on preliminary findings  
157 from our research group.<sup>69</sup>

158 **Lignin Nanoparticles (LNPs) preparation.** LNPs were synthesized through a simple  
159 environmentally friendly anti-solvent precipitation method. Initially, each LMPs fraction was  
160 dissolved in an 80% v/v EtOH/H<sub>2</sub>O solution with ultrasonic treatment for 1h to ensure complete  
161 lignin solubilization at a concentration of 30 mg/mL. The resulting solution sustained vacuum  
162 filtration using a 0.45 µm nylon filter to eliminate potential aggregates, which represented between  
163 0.9 and 3.1% of total solubilized mass for beech, spruce and wheat straw compared with 6.8% for  
164 KL. The production of LNPs involved a KF Technology® NE-1010 syringe pump, which allowed  
165 the controlled precipitation of the lignin solutions into ultrapure water with agitation at 1000 rpm  
166 and a temperature of 20 °C. The process maintained a consistent flow rate of 100 mL/min until  
167 achieving a final concentration of 3 mg/mL under a 500-rpm magnetic agitation. The resulting  
168 suspensions were predominantly aqueous, with a composition of 91/9 H<sub>2</sub>O/EtOH v/v. Suspensions  
169 were stored at 4 °C before further analysis.

170 **Elemental analysis.** Thermo Finnigan Flash EA® 112 Series was used to perform sulphur  
171 elemental analysis. Samples combustion (1.5 mg) was performed for 15 s at high temperature

172 (1000 °C) under oxidizing atmosphere and in the presence of tungstic anhydride. Gaseous products  
173 produced (H<sub>2</sub>O, SO<sub>2</sub>, CO<sub>2</sub>, NO<sub>x</sub>) were reduced to N<sub>2</sub> in the presence of copper and then were  
174 analyzed by gas chromatography. The percentage of sulfur present in the compound was calculated  
175 by using Eager 300 software.

176 **Size Exclusion Chromatography (SEC).** SEC analyzed LMPs fractions for molecular weight  
177 distributions and averages. Each lignin sample, initially dissolved in 10 mM NaOH at 5 mg/mL  
178 under 24 h magnetic agitation, was filtrated with 0.45 µm PTFE filters. Shimadzu Prominence™  
179 chromatography outfitted with a Shimadzu SPD-20A UV detector (280 and 254 nm), a refractive  
180 index detector (RID, Shimadzu RID-20A), and Shodex™ GPC KF-806L and Phenogel™ 00H-  
181 0442-K0 columns, was used. The separation occurred at 35 °C, with elution using 10 mM NaOH  
182 at a flow rate of 0.4 mL/min. The calibration curve was plotted using Aligent Technologies®  
183 GPC/SEC calibration kits (Aligent PL2090-0101) and Steinmetz et al.<sup>70</sup> method's.

184 **Nuclear Magnetic Resonance (NMR).** The examination of the lignin structure involved both  
185 Heteronuclear Single Quantum Coherence (HSQC) and <sup>31</sup>P NMR. In a concise procedure for  
186 HSQC, 100 mg of purified and dried LMPs was dissolved in 700 µL of dimethyl sulfoxide-d<sub>6</sub>  
187 (DMSO-d<sub>6</sub> 99.8%). Spectra were acquired using the Bruker® Avance III 400 MHz spectrometer  
188 at 50 °C with a relaxation delay of 25 seconds. For <sup>31</sup>P NMR, hydroxyl group content was  
189 determined following published methodology<sup>71</sup> where 25 mg of purified LMPs was dissolved in  
190 400 µL of pyridine/deuterated chloroform (1.6/1 v/v). A mixed solution (A) of Chromium (III)  
191 Acetylacetonate 97% (3.6 mg/mL) and Cyclohexanol (4.0 mg/mL of A) served as the relaxation  
192 reagent and internal standard. The solution was derivatized with 50 µL of 2-Chloro-4,4,5,5-  
193 tetramethyl-1,3,2-dioxaphospholane (TMDP), vortexed, and analyzed using the Bruker® Avance

194 III HD 300 MHz spectrometer at 25 °C with a 2 s relaxation delay. NMR data were processed  
195 using Topspin<sup>®</sup> 4.1.0 software (Bruker Bio Spin).

196 **Scanning Electron Microscopy (SEM).** First set of LMPs images were determined using  
197 Hitachi<sup>®</sup> TM3000 Scanning Electron Microscopy (SEM). 2 mg of LMPs each powder was applied  
198 onto sample holder for metallization using a Polaron SC7620 Quorum<sup>®</sup> Sputter Coater. All images  
199 were taken at an accelerating voltage of 15 kV. Then, second set of images were taken using a  
200 JEOL<sup>®</sup> JSM-IT200.

201 **Dynamic Light Scattering (DLS).** Malvern<sup>™</sup> Zetasizer ULTRA instrument was used to determine  
202 the size distribution, size average, polydispersity index (PDI), and  $\zeta$ -potential of the prepared LNPs  
203 suspensions. LNPs suspensions were analyzed immediately after precipitation at 25 °C by  
204 complete optical PS cells with a volume of 1.5 mL. Triplicate measurements were recorded in DLS  
205 mode at an angle of 174 °.  $\zeta$ -potential analyses were performed using the same instrument,  
206 employing special folded capillary Zeta cells (DTS 1070) at 25 °C. Solid LNPs were obtained by  
207 freeze drying using a BILON<sup>®</sup> FD-1A-50 freeze dryer.

208 **Transmission Electron Microscopy (TEM).** LNPs images were captured through a FEI Philips<sup>®</sup>  
209 CM200 Transmission Electron Microscope (TEM), operating at an accelerating voltage of 160 kV.  
210 The samples were directly prepared by applying a drop of LNPs suspension (3 mg/mL) without  
211 contrasting agents onto a TEM grid and dried for 30 min.

212 **Lignin-based sunscreens preparation and study.** Every lignin-based sunscreen formulation was  
213 generated by mixing LMPs or LNPs powder with corresponding sunscreen or pure cream at 1, 5  
214 and 10 wt% at 400 rpm for 14h in a dark room. After blending, 37.5 mg of lignin-based sunscreens  
215 were applied onto clean 7.5x2.5 cm quartz plate of 2 mm thickness to respect International Sun

216 Protection (SPF) Test Method conditions of 2.0 mg/cm<sup>2</sup>. The sunscreen was carefully spread  
217 across the entire surface by gently rubbing the slide with a nitrile finger cot. Subsequently, the  
218 sample was left to dry for 15 minutes in a dark room before UV transmittance measurements. The  
219 UV transmittance of lignin-based sunscreens was measured using Shimadzu® UV-1900i  
220 spectrophotometer. For each lignin-based sunscreen, a minimum of 5 samples were prepared and  
221 measurements were repeated at least 3 times. Transmittance measurements were accumulated in  
222 the wavelength spectrum from UVB (290-320 nm) to UVA (320-400 nm). Finally, SPF value was  
223 calculated according to the following equation :

$$224 \quad SPF = \frac{\sum_{290}^{400} E_{\lambda} S_{\lambda}}{\sum_{290}^{400} E_{\lambda} S_{\lambda} T_{\lambda}}$$

225 where  $E_{\lambda}$  = CIE erythral efficiency spectrum,  $S_{\lambda}$  = solar irradiance spectrum, and  $T_{\lambda}$  =  
226 transmittance spectrum of the sample. The values of  $E_{\lambda}$  and  $S_{\lambda}$  are constants and they were  
227 determined by Sayre et al.<sup>72</sup>.

## 228 RESULTS AND DISCUSSION

229 The objective of this study was to generate tailored LNPs from various feedstock through eco-  
230 friendly processes and analyze the impact of these parameters on the lignin-based sunscreens  
231 performance.

232 **LMPs extraction and characterization.** In order to overcome current limitations of lignin from  
233 pulping processes, i.e. its extraction using toxics solvents and its relatively-high sulfur  
234 composition, we used ethanol organosolv pretreatment without acid catalysis. This method has the  
235 advantage of generating clean and pure LMPs with chemical structure that closely matching that  
236 of native one. In addition, by starting from native biomass, we carefully select diverse species

237 (hardwood, softwood, herbaceous material) with various lignin chemical structures represented by  
 238 G, S, and H units, what is crucial for nanometric size reduction and future UV-absorbing properties  
 239 in the lignin-based sunscreens (**Figure 1**). Therefore, in this present work, LMPs extraction and  
 240 structural features results investigated by NMR ( $^{31}\text{P}$ , and HSQC) and SEC techniques are listed in  
 241 **Table 1**. Consequently, organosolv process provides the advantage of combining very pure lignin  
 242 (93.0%, 96.1%, and 93.3% for beech, spruce, and wheat straw respectively), with high extraction  
 243 yields depending on biomass species (69.7%, 35.9%, and 44.8% for beech, spruce, and wheat  
 244 straw respectively and based on raw lignin biomass content) and absence of sulfur compared to  
 245 commercial kraft lignin (1.8%) which is key factor for prospective industrial purposes.

246 Concerning average LMPs molecular weight ( $M_w$ ) results in **Table 1** and **Table S1**, it appeared  
 247 that organosolv delignification treatment has led to  $M_w$  reduction conform with lignin breakdown.  
 248 Furthermore, all three lignin's extracted using the organosolv process had a lower average  $M_w$   
 249 (20.8, 15.7, and 17.2 kDa for beech, spruce and wheat straw respectively) than the lignin derived  
 250 from kraft process (29.4 kDa). This result suggests that both type of feedstock and the extraction  
 251 process parameters play a part in lignin reaction mechanisms such as depolymerization and  
 252 recondensation.

253 **Table 1.** Results from LMPs characterization for beech, spruce, wheat straw, and kraft lignin.

LMPs characterizations	Organosolv 200°C 60min 60/40 EtOH/H <sub>2</sub> O (v/v)			Kraft
	Beech	Spruce	Wheat straw	
Extraction yields (wt%)	69.7 ± 0.8	35.9 ± 1.2	44.8 ± 0.4	
Purity (%)	93.0 ± 0.4	96.1 ± 0.1	96.3 ± 0.7	91.5 ± 0.3

Sulphur content (%)	< 0.05	< 0.05	< 0.05	1.8
<b>Size exclusion chromatography (SEC) – Average Molecular weight (M<sub>w</sub>)</b>				
M <sub>w</sub> (kDa)	20.8	15.7	17.2	29.4
<b><sup>31</sup>P Nuclear Magnetic Resonance (NMR) – Hydroxyl groups (mmol.g<sup>-1</sup>)</b>				
<b>Total -OH</b>	4.19	3.71	2.94	4.62
<b>Aliphatic -OH</b>	2.26	1.71	1.27	1.68
<b>Phenolic -OH</b>	1.93	1.86	1.44	2.53
Syringyl	1.18	0.14	0.59	0.36
Guaiacyl	0.74	1.59	0.61	2.17
p-Hydrophenyl	0.01	0.13	0.24	0
<b>COOH</b>	0	0.14	0.23	0.41
<b>Heteronuclear single quantum coherence (HSQC) NMR spectroscopy – Linkages (%)</b>				
<b>β-O-4 (%)</b>	25.28	17.89	16.09	9.65
<b>β-5 (%)</b>	3.94	13.71	3.94	2.44
<b>β-β (%)</b>	6.76	3.06	1.40	3.72
<b>S/G</b>	1.87	0	1.03	0

254 LMPs extraction (wt%) yields are based on raw lignin biomass content. Results includes lignin purity (%), sulfur content (%), average Mw from  
255 SEC but also the quantification of functional groups, side chains, and aromatic regions from <sup>31</sup>P and HSQC NMR.

256 Precisely, in order to further investigate the chemical structure of the different recovered LMPs,  
257 <sup>31</sup>P and two-dimensional HSQC NMR measurements were utilized in this work. According to  
258 literature<sup>73</sup> **Table 1** showed the structural assignments and amounts (mmol.g<sup>-1</sup> of lignin) of main  
259 signals of <sup>31</sup>P NMR for the phosphitylated LMPs. By considering former results of milled wood  
260 lignin (MWL) <sup>31</sup>P spectrums from Brosse et al.<sup>74</sup> and Qian et al.<sup>71</sup>, we observed a significant

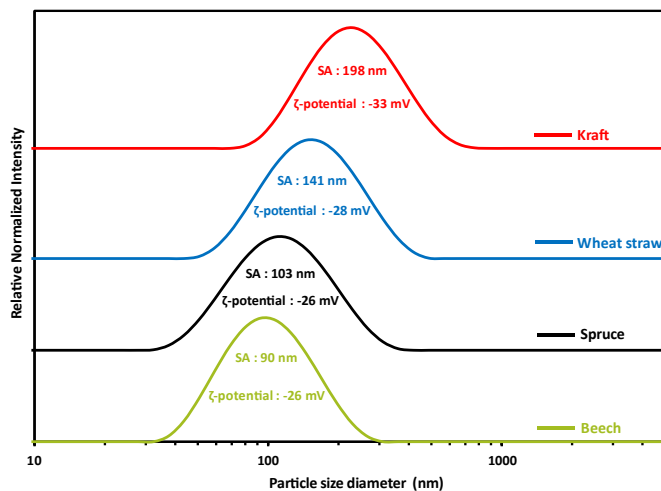
261 increase in phenolic -OH groups due to the  $\beta$ -O-4 aryl ether acidolytic scission. Kraft lignin  
262 appears to undergo higher recondensation according to  $^{31}\text{P}$  NMR results with the wide increase of  
263 the guaiacyl -OH amount compared to spruce organosolv lignin. Then, according to Crestini et  
264 al.<sup>75</sup> and Wang et al.<sup>76</sup> analysis, HSQC NMR was conducted in order to investigate side chains and  
265 aromatic regions change ratio ( $\beta$ -O-4,  $\beta$ -5,  $\beta$ - $\beta$  and S/G amount in %) and shown in **Table 1**. Milled  
266 wood results for extracted lignin's in **Table S1** confirmed that organosolv pretreatment has led to  
267 lignin depolymerization highlighted by the  $\beta$ -O-4 acidolytic breakdown. The elevated S/G ratios  
268 observed in both beech and wheat straw also indicate lignin depolymerization. Concerning  
269 organosolv spruce lignin and kraft lignin, results indicate that kraft process has a more severe  
270 influence on the chemical structure by promoting depolymerization and recondensation.

271 Results from **Table 1** suggest that, independently of the feedstock type, organosolv allows the  
272 extraction of a lignin that is close to the native one with less depolymerization and recondensation  
273 compared with the kraft process. Moreover, as expected with Adamczyk et al.<sup>52</sup> and Siika-aho et  
274 al.<sup>77</sup> studies, results from **Table 1** indicated that delignification and lignin depolymerization is  
275 easier for both hardwood and herbaceous material compare to softwood for same process  
276 severities. Nevertheless, herbaceous material continues to pose processing challenges due to its  
277 low density and important ashes content compare to hardwood and softwood biomass,  
278 necessitating specific optimizations for efficient fractionation step. This part also shows the  
279 importance of the starting biomass in terms chemical composition and lignin structure for the  
280 optimization of the produced LNPs properties (size, shape and UV absorption capacity) regarding  
281 these results.

282 **LNPs production and characterization.** In previous work, lignin size reduction has been widely  
283 implemented by hazardous precipitation with toxic or explosive solvents such as tetrahydrofuran

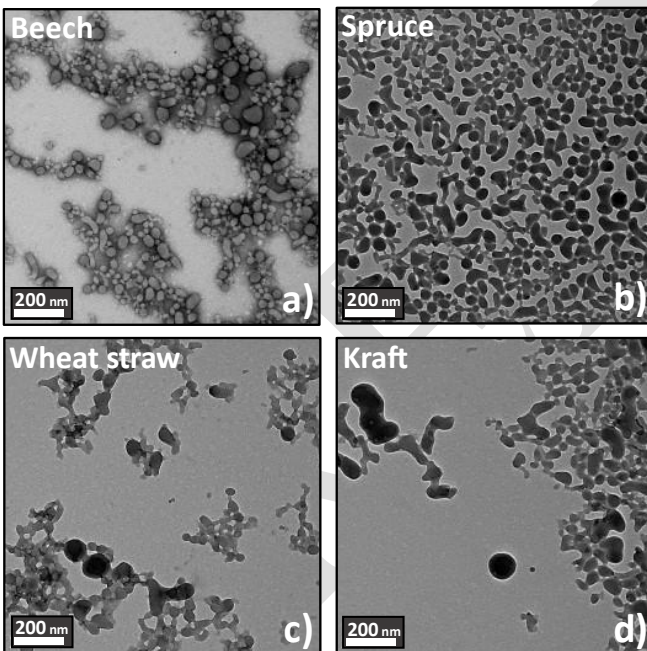
284 (THF), pyridine or dimethyl sulfoxide (DMSO).<sup>27</sup> Recent studies have focused on the importance  
285 of precipitation parameters (polymer concentration,<sup>58,78,79</sup> solvent and anti-solvent,<sup>80-82</sup>  
286 temperature<sup>81</sup> and mixing forces<sup>83-86</sup>) concerning the LNPs formation mechanisms driven by both  
287 lignin chemical molecules interactions<sup>60,87-89</sup> ( $\pi$ - $\pi$  staking and hydrophobic groups such as the  
288 phenylpropanoid units) and the supersaturation theory<sup>90,91</sup>. Based on this work, we successfully  
289 established an optimized method with interesting LNPs production yields and properties (size,  
290 shape, stability and polydispersity) but also but also prioritized environmental considerations by  
291 utilizing only ethanol and water as solvents. More precisely, we performed anti-solvent  
292 precipitation using an 80% v/v EtOH/H<sub>2</sub>O of LMPs at a concentration of 30 mg/mL. The process  
293 involved a consistent flow rate of 100 mL/min and a magnetic agitation of 500-rpm to produce 3  
294 mg/mL stable nano-suspensions. The size distribution, size average, and  $\zeta$ -potential of the prepared  
295 LNPs suspensions were analyzed using Malvern™ Zetasizer as shown in Fig. 2. Uniform size  
296 distributions were observed in all suspensions, with LNPs size results (repartition and average)  
297 decrease in order kraft > wheat straw > spruce > beech lignin. Indeed, beech suspension features  
298 the smaller size distribution, with values between 30 and 300 nm for an average size of 90 nm. By  
299 comparing with other organosolv-isolated lignin, size average results are nearly equivalent with  
300 particles size of 103 nm and 141 nm for spruce and wheat straw respectively. The distinction is  
301 more pronounced with kraft lignin, which forms particles with an average size of 198 nm, i.e. twice  
302 the size found for beech lignin nanoparticles. Results in **Figure 2** support the theory of LNPs  
303 formation mechanisms partly driven by lignin chemical structure interactions, once again  
304 underlining the crucial importance of selecting the appropriate biomass for further industrial  
305 integration. Based on the work of Beisl et al.<sup>92</sup>, the major limitations associated with anti-solvent  
306 precipitation are the environmental concerns related to the solvents used and the relatively low

307 concentrations achievable in suspensions. Our innovative approach prioritizes eco-friendly  
308 solvents, highlighting that lignin obtained through optimized organosolv methods achieves a more  
309 favorable particle size distribution than traditional methods. In **Figure 2**, size distributions of  
310 organosolv-isolated lignins (beech, spruce, wheat straw) reveal limitations for cosmetic  
311 applications, with 25 to 50% of particles below the 100 nm threshold. Despite this, the findings  
312 enable the production of more concentrated suspensions with a similar size distribution, enhancing  
313 the versatility of our process. **Figure 2** also showed the  $\zeta$ -potential of the prepared LNPs  
314 suspensions. Results revealed a highly negative  $\zeta$ -potential for all suspensions (-26 to -33 mV)  
315 maintaining self-repulsion and electrostatic stability over time in water (size variation between 3  
316 to 10% after 90 days).



317  
318 **Figure 2.** Results of the particle size distribution obtained from production and analysis triplicate  
319 according to fractionation process and lignin type determined by DLS measurements. SA: size  
320 average. Anti-solvent precipitation parameters were : LMPs concentration : 10 mg/mL. Addition  
321 rate : 40 mL/min. Anti-solvent composition : 100 % water. Dilution ratio : 1/10. T °C : 20 °C.  
322 Stirring speed : 400 rpm.

323 TEM microscopic analyses were employed to enhance the characterization of LNPs properties in  
324 **Figure 3**, providing visual insight into the stabilized particles shapes. First, we noticed a  
325 correlation between particles size distribution results and TEM images for every lignin type. In  
326 this case, beech-sourced particles were spherical and isotropic, with a distribution almost identical  
327 to that of DLS measurements. In contrast, particles from other feedstock especially wheat straw  
328 and spruce from kraft process assume irregular shapes, characterized by a dense core enveloped in  
329 a fluffy outer wreath. Comparing kraft and spruce organosolv-sourced lignins, images also  
330 indicates that the process severity impacting the lignin chemical structure results in different  
331 nanoparticles properties in terms of size and shape.



332

333 **Figure 3.** TEM images of the suspension generated according to fractionation process and biomass  
334 type. Bottom row of TEM images = 200 nm

335 The multiparameter mechanism behind the formation of lignin nanoparticles in the anti-solvent  
336 system can be partially explained by considering the well-documented amphiphilic nature of lignin  
337 polymer, as extensively done in literature.<sup>59,93–95</sup> Higher phenolic hydroxyl and carboxyl content  
338 enhance hydrophilicity, while non-covalent  $\pi$ - $\pi$  interactions contribute to hydrophobicity,  
339 especially in lignin with more S units (S > G > H). Consequently, hydrophobic lignin solutions  
340 guided by  $\pi$ - $\pi$  stacking and the S/G ratio, yield smaller and more spherical LNPs.<sup>82</sup> Conversely,  
341 hydrophilic solutions, such as the kraft sample, lead to the formation of larger more irregular  
342 nanoparticles by reducing the aggregation phenomenon as the self-assembly process involves the  
343 hydrophobic core and the hydrophilic components twist towards the surface (**Table 1, Figure 2**  
344 **and Figure 3**).<sup>87</sup> Finally, concerning LNPs production yields, the established nanoprecipitation  
345 process is very interesting because only dependent of the lignin solubilization and suspensions  
346 lyophilization performances. For lignin solubilization in ethanol aqueous mix, mass yields were  
347 respectively of 96.9, 99.1 and 97.2% for beech, spruce and wheat straw. About lyophilization,  
348 mass loss was between 4.9 and 6.8%, generating global yields from raw biomass waste to  
349 nanolignin powder of 63.8, 33.8 and 40.6% for beech, spruce and wheat straw respectively (based  
350 on initial raw lignin biomass content).

351 **Lignin-based sunscreens analysis.** For this part, diverse samples of lignin-based sunscreens were  
352 prepared following the outlined procedure. Our investigations focused on assessing the impact of  
353 various parameters on the UV-absorption sunscreen efficacy, including particles concentration,  
354 lignin chemical structure (feedstock and isolation process) and particles size. In each formulation,  
355 lignin particles were directly mixed into commercial creams with varying sun protection factors  
356 (SPF 0, SPF 10, SPF 30). The results were also compared with pure SPF 10 and SPF 30  
357 commercial sunscreens as references. Transmittance and the related SPF-value of the lignin-based

358 sunscreens were measured in the UVA (320-400 nm) and UVB (280-320 nm). The different results  
359 were summarized in **Figure 4**, **Table 2**, **Figure S1**, **Figure S2** and **Figure S3**.

360 First, **Figure 4** and related **Table 2** results indicated that the pure cream was UV-filters free with  
361 the maximum transmittance of 95-90% corresponding to a SPF of 1.08. Then, **Figure 4A**  
362 confirmed former results from literature<sup>19,20,22,24,26,28,96</sup> with the decrease of UV transmittance  
363 linked to an increase of SPF values when LMPs was added to pure cream regardless of the lignin  
364 type or biomass feedstock. The SPF values of the 1 wt% lignin-based pure cream were ranged  
365 from 1.27 to 1.66 with the lower transmittance in both UVA and UVB area for the organosolv-  
366 wheat straw lignin (OWS). Huge gap was observed with 5 wt% of lignin concerning kraft and  
367 organosolv-spruce (OS) compare to organosolv-beech (OB) and wheat straw lignins (SPF values  
368 from 2.51 and 7.33). Indeed, results from 5 wt% lignin-based OWS and OB pure cream were  
369 practically equivalent from the kraft and OS 10 wt% (Figure 4A). For 10 wt% amount, OWS  
370 standout from other preparation with SPF of 25.30 compare to 11.24, 9.65 and 8.85 for OB, OS  
371 and kraft lignin respectively.

372

373

374

375

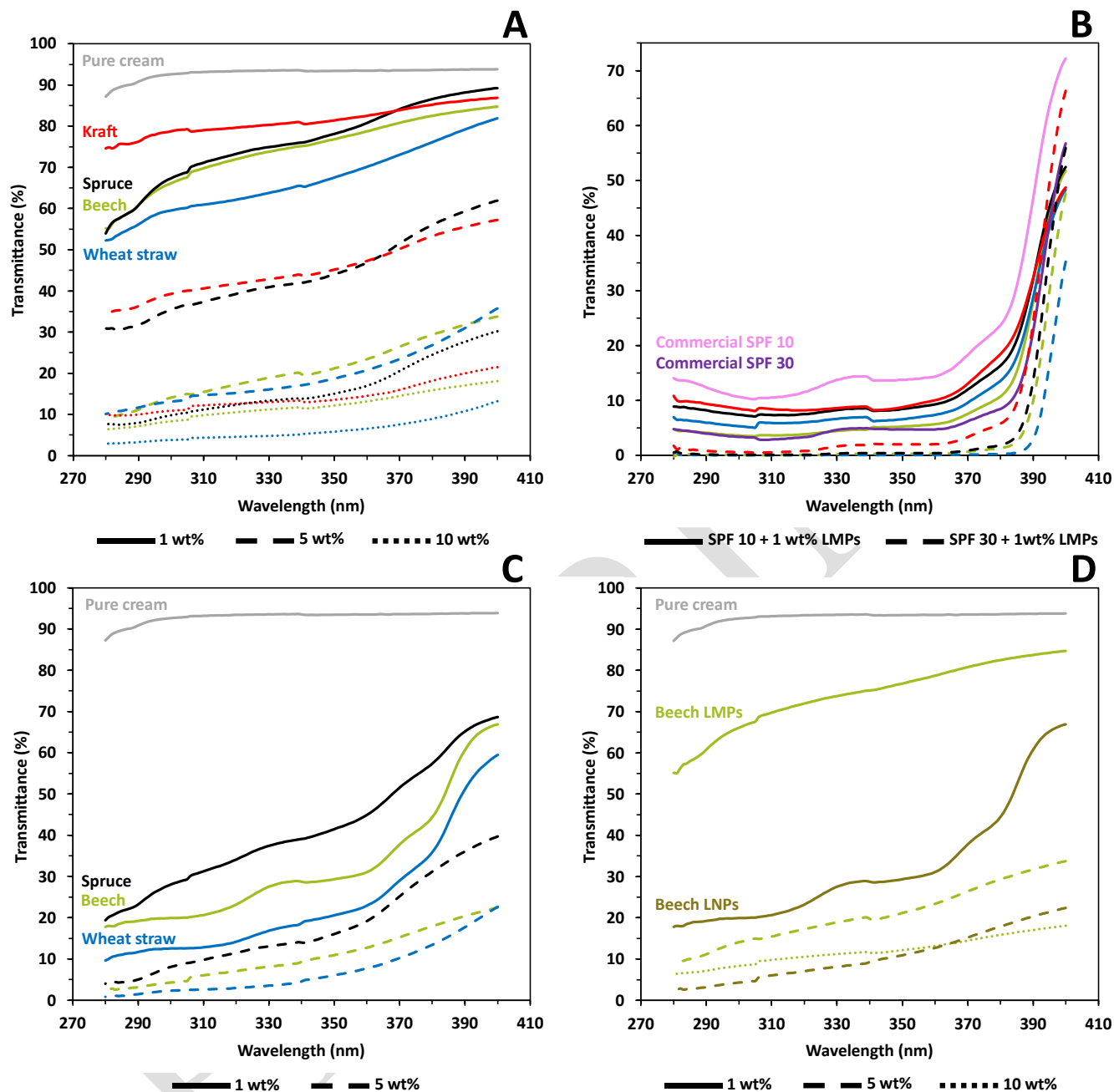
376

377

378

379

380



381 **Figure 4.** UV transmittance results in UVA and UVB area from lignin macro and nanoparticles  
 382 blended with pure cream and sunscreens. A) UV transmittance of pure cream mixed different  
 383 amount of LMPs. In grey: pure cream. In green: beech. In black: spruce. In blue: wheat straw. In  
 384 red: kraft. In solid line: 1 wt%. In coarse dotted line: 5 wt%. In fine dotted line: 10 wt%. B) UV  
 385 transmittance of commercial SPF 10 (pink) and SPF 30 (purple) mixed with 1 wt% of LMPs. In

386 green: beech. In black: spruce. In blue: wheat straw. In red: kraft. In solid line: commercial SPF  
 387 10 sunscreen + LNPs. In coarse dotted line: commercial SPF 30 sunscreen + LNPs. C) UV  
 388 transmittance of pure cream mixed different amount of LNPs. In grey: pure cream. In green: beech.  
 389 In black: spruce. In blue: wheat straw. In solid line: 1 wt%. In coarse dotted line: 5 wt%. D) UV  
 390 transmittance of pure cream mixed different amount of beech LNPs vs LNPs. In light green:  
 391 LNPs. In dark green: LNPs. In solid line: 1 wt%. In coarse dotted line: 5 wt%. In fine dotted line:  
 392 10 wt%. Other results available in ESI.

393

394 **Table 2.** Measured SPF values for lignin-based pure cream and commercial sunscreens.

LNPs (wt%)	0 <sup>a</sup>	Beech			Spruce			Wheat straw			Kraft		
		1	5	10	1	5	10	1	5	10	1	5	10
Pure Cream	1.08	1.48	6.77	11.24	1.45	2.76	9.65	1.66	7.33	25.30	1.27	2.51	8.85
	± 0.02	± 0.03	± 1.09	± 0.24	± 0.05	± 0.13	± 1.23	± 0.02	± 1.37	± 4.31	± 0.02	± 0.65	± 1.21
LMPs (wt%)	0 <sup>b</sup>	1		5		1		5		1		5	
Commercial SPF 10	9.39	27.43		50+		13.70		26.17		18.29		50+	
	± 0.53												
LMPs (wt%)	0 <sup>c</sup>	1			1			1			1		
Commercial SPF 30	30.93	50+			50+			50+			50+		
	± 4.97												
LNPs (wt%)	0 <sup>a</sup>	Beech		Spruce		Wheat straw							
		1	5	1	5	1	5	1	5	1	5	1	5
Pure Cream	1.08	4.93 ± 0.53		20.17 ± 2.20		3.41 ± 0.96		11.39 ± 1.32		7.88 ± 0.84		41.97 ± 7.38	

	± 0.02				
--	-----------	--	--	--	--

395 <sup>a</sup>Commercial pure cream without UV-shielding properties. <sup>b</sup>Commercial sunscreen with SPF 10 without lignin addition. <sup>c</sup>Commercial sunscreen  
396 with SPF 30 without lignin addition.

397 Close trends were therefore observed for hardwood and herbaceous species: transmittance  
398 decrease related to UV-shielding follow the lignin concentration of the lignin-based cream.  
399 Conversely, for softwood specie the UV-shielding evolution is more gradational depending of  
400 the total amount of lignin inside the cream. Our better results compared to literature<sup>19,20,22,26</sup> can  
401 be explained by the use of organosolv lignin demonstrated by Qian et al.<sup>20</sup> to be the most suitable  
402 for high SPF cream, but also by our effective homogeneity (**Figure S1**) even with macrolignins  
403 compare to Zhang et al.<sup>96</sup> work.

404 Today, if the brown characteristic color of lignin is still a problem, the solution may lie in the use  
405 of this natural organic filter as a complement of current filters to reduce their proportions.  
406 Therefore, we also investigate the enhancement of commercial SPF 10 and SPF 30 sunscreens  
407 with LMPs. Results in **Figure 4B** and **Figure S2** indicated that LMPs improve both commercial  
408 SPF 10 and SPF 30 sunscreens. The same trends as before were observed, hardwood and  
409 herbaceous LMPs exhibited better UV-shielding properties with the transmittance of SPF 10 + 1  
410 wt% closely match the one of the commercial SPF 30 sunscreens (SPF values of 18.29 and 27.43).  
411 For softwood LMPs, it's only for a 5 wt% that the transmittance of the SPF 10 corresponds to the  
412 one of the SPF 30 sunscreens (SPF values of 22.65 and 26.17). In the case of adding 1 wt% of  
413 LMPs in the commercial SPF 30 lotion, the UV-shielding was total with transmittances close to 0  
414 and very high related SPF (more than 100 but indexed 50+ for a concrete meaning).

415 The enhanced properties observed in a cream blended with lignin can be attributed to two potential  
416 factors. Firstly, the chemical composition of the UV filter and its interactions with the constituents

417 of the cream play a crucial role as it was previously demonstrated. Additionally, the size and  
418 geometry of the adding filter also contribute to these improvements. Consequently, we prepared  
419 in **Figure 4C and Figure 4D**, LNPs-based pure cream 1 wt% and 5 wt% from OB, OS and OWS  
420 lignins in order to quantify the reduction size impact over the pure cream properties (UV-shielding  
421 and color). Once again, increasing the amount of lignin improved the blended pure cream  
422 properties with an advantage herbaceous > hardwood > softwood. Indeed, SPF results for the 1  
423 wt% LNPs-based pure cream were 7.88, 4.93 and 3.41 respectively for wheat straw, beech, spruce.  
424 When the creams were prepared with 5 wt% of LNPs, the SPF reached values of 41.97, 20.17 and  
425 11.39 for the same extracted lignin's. By comparing UV-shielding properties between LMPs and  
426 LNPs prepared pure creams in **Figure 4D and Figure S3**, the lignin particle size impact was  
427 demonstrated. Indeed, macro to nano scale reduction improved the UVB average transmittance of  
428 pure creams prepared with the same lignin wt% by between 2.5 and 6.5. Thus, close UVB average  
429 transmittances were observed between LMPs 5 wt% - LNPs 1 wt% but also LMPs 10 wt% - LNPs  
430 5 wt%, which consequently revealed a correspondent brown color reduction for LNPs-based pure  
431 cream (**Figure S1**).

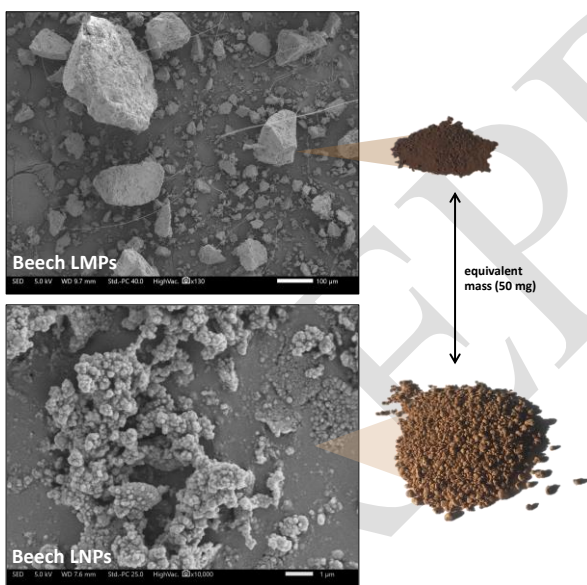
432 **Factors affecting lignin UV-shielding properties.** It is generally accepted that there are several  
433 factors affecting the UV-blocking performances of lignin polymer. These factors manifest in two  
434 different forms according to Zhang et al.<sup>97</sup> : (1) the intrinsic chemical structure of lignin relied to  
435 biomass nature and (2) the extrinsic factors including the size, shape and purity of the lignin  
436 particles determined by the extraction and nanoparticles fabrication processes.

437 (1) Lignin UV-shielding properties are related to chromophore functional groups and  
438 especially phenolic hydroxyl groups.<sup>22,27,31,96-98</sup> Guo et al.<sup>99</sup> previously demonstrated that  
439 the S phenolic group as the stronger UV-absorbing properties due to the additional

440 methoxyl group compared to G and H units (**Figure 1**); consequently enhancing the  
441 abundance of free electron pairs from the oxygen atoms. Part of our results are in line with  
442 these explanations: beech and wheat straw biomass who present most advantageous  
443 chemical structures (high S/G phenolic hydroxyl content i.e. high methoxyl content and  
444 darker color<sup>24</sup>) had greater UV-shielding properties compare to spruce lignin. It was  
445 previously demonstrated by Wang et al.<sup>26</sup> that lignin chemical structure remains unchanged  
446 with the nanoprecipitation process which explains why the same trends can be observed  
447 between sunscreens prepared with LMPs and LNPs. However, the observation that wheat  
448 straw lignin exhibited superior stronger UV-shielding properties over beech lignin suggests  
449 that while methoxyl groups and phenolic units may be predominant, they do not fully  
450 account for all aspects of the lignin enhanced UV protection. Other chromophores in lignin  
451 like the quinones or -CH=CH-, -C=C- and -C=O bonds as well as the M<sub>w</sub> can contribute to  
452 UVB and UVA absorbance.

453 (2) Although the extrinsic properties of lignin are often given less consideration, particle size,  
454 shape and purity can be modified by processes and are also important factors that can  
455 explain UV-absorption properties. First, relative highest level of impurities (7%) were  
456 found in beech lignin compare to other organosolv-extracted lignins (respectively 3.7 and  
457 3.9% for wheat straw and spruce), which may reduce UV-shielding properties to a greater  
458 extent. In case of kraft, the 9.5% of impurities coupled with the 1.8% sulfur presence can  
459 also contribute to lower UV absorption despite a large amount of aromatic rings.  
460 Concerning lignin particle size and morphology, recent studies<sup>22,100</sup> showed that lignin  
461 nanoparticles compared to macroparticles have higher specific surface area, higher  
462 transparency, better dispersibility and consequently better UV-shielding properties per

463 weight (**Figure S1 and Figure 5**). Indeed, lower size induce higher specific surface area,  
464 thus allowing more chromophores for the same weight, allowing better UV-shielding  
465 properties in line with lighter color, better dispersion inside the sunscreen and also lower  
466 overall cytotoxicity (**Figure S1**). Our results have indeed demonstrated previous  
467 explanations with a general increase in UVB average transmittance between 2.5 and 6.5  
468 with same lignin but different size scale. For particle shape, Tan et al.<sup>68</sup> showed that  
469 spherical design provide larger surface area because of the minimum packing density  
470 compare with other forms, thus allowing higher chromophores concentration which can  
471 boost UV absorption properties.



472  
473 **Figure 5.** SEM images of LMPs (top) and solid LNPs (bottom) from beech lignin with specific  
474 surface area for same mass. Bottom row of SEM images = 100 µm for LMPs and 1 µm for LNPs.

475  
476  
477  
478

## 479 CONCLUSIONS

480 To conclude, we successfully produce various sunscreen with macro and nanoparticles of lignin  
481 biopolymer as natural UV-filter in an ecological and simple way from different biomass waste and  
482 extraction processes. With this, we were able to highlight and quantify the importance of lignin's  
483 intrinsic (chemical structure) and extrinsic parameters (lignin extraction and LNPs fabrication)  
484 over furthers UV-shielding properties of sunscreens. First, with regard to chemical structures,  
485 grasses and hardwoods exhibit a higher prevalence of methoxyl groups, recognized as the primary  
486 units influencing UV absorption properties, resulting in a 2.5 times performances improvement  
487 compared to softwoods regardless of particles size and concentration. Then, reducing particle size  
488 from macro to nano scale enhances dispersion, increases specific surface area, and consequently  
489 amplifies UV absorbance, achieving color reduction and between 2.5 and 6.5-fold improvement  
490 independent of lignin nature and concentration. From this, sunscreen formulated with 5 wt% LNPs  
491 from wheat straw achieved an SPF value of 41.97, approaching that of high-protection lotions.  
492 When added to commercial sunscreens, lignin boost performances while reducing synthetic filters  
493 concentration with 50+ protection from SPF 10 lotion with 5 wt% of LNPs. This study presents a  
494 straightforward approach for lignin polymer valorization with the formulation of green next-  
495 generation sunscreens using LNPs, exhibiting excellent UV-absorbing properties.

496

## 497 ASSOCIATED CONTENT

498 **Supporting Information.** The supporting information is available free of charge on the ACS  
499 Publication website. The following files are available free of charge.  
500 MWL and main lignin linkages (%); Appearance of each produced sunscreen; UV transmittance

501 of commercial SPF 10 sunscreen mixed with 5 wt% of LMPs; UV transmittance of pure cream  
502 mixed different amount of LMPs and LNPs.

### 503 AUTHOR INFORMATION

#### 504 **Corresponding Author**

505 Isabelle Ziegler-Devin

506 E-mail : [isabelle.ziegler-devin@univ-lorraine.fr](mailto:isabelle.ziegler-devin@univ-lorraine.fr)

#### 507 **Author Contributions**

508 Victor Girard: Conceptualization, Analysis, Investigation, Writing - original draft. Hubert  
509 Chapuis: Project administration, Supervision, Investigation. Nicolas Brosse: Writing - review &  
510 editing. Nadia Canilho: Investigation, Methodology, Analysis. Stéphane Parant: Methodology,  
511 Analysis. Laurent Marchal-Heussler: Investigation, Methodology, Analysis. Isabelle Ziegler-  
512 Devin: Project administration, Funding acquisition, Supervision, Methodology, Investigation,  
513 Analysis.

#### 514 **Funding Sources**

515 The authors thank the French National Research Agency and the Grand Est Region for their  
516 financial support provided through the ARBRE Laboratory of Excellence (ARBRE; grant ANR-  
517 11-LABX-0002-01).

#### 518 **Notes**

519 The authors declare no competing financial interest.

### 520 ACKNOWLEDGMENT

521 The authors also express their deep appreciation to the Plateforme PhotoNS of the L2CM  
522 Laboratory, University of Lorraine, and the CC3M of the IJL Laboratory, University of Lorraine.

## 523 REFERENCES

- 524 (1) Diaz, J. H.; Nesbitt, L. T. Sun Exposure Behavior and Protection: Recommendations for  
525 Travelers. *J Travel Med* **2013**, *20* (2), 108–118. [https://doi.org/10.1111/j.1708-](https://doi.org/10.1111/j.1708-8305.2012.00667.x)  
526 [8305.2012.00667.x](https://doi.org/10.1111/j.1708-8305.2012.00667.x).
- 527 (2) Young, A. R.; Narbutt, J.; Harrison, G. I.; Lawrence, K. P.; Bell, M.; O'Connor, C.; Olsen, P.;  
528 Grys, K.; Baczynska, K. A.; Rogowski-Tylman, M.; Wulf, H. C.; Lesiak, A.; Philipsen, P. A.  
529 Optimal Sunscreen Use, during a Sun Holiday with a Very High Ultraviolet Index, Allows  
530 Vitamin D Synthesis without Sunburn. *Br J Dermatol* **2019**, *181* (5), 1052–1062.  
531 <https://doi.org/10.1111/bjd.17888>.
- 532 (3) Gilbert, E.; Pirot, F.; Bertholle, V.; Roussel, L.; Falson, F.; Padois, K. Commonly Used UV  
533 Filter Toxicity on Biological Functions: Review of Last Decade Studies. *Int J Cosmet Sci*  
534 **2013**, *35* (3), 208–219. <https://doi.org/10.1111/ics.12030>.
- 535 (4) Schneider, S. L.; Lim, H. W. A Review of Inorganic UV Filters Zinc Oxide and Titanium  
536 Dioxide. *Photoderm Photoimm Photomed* **2019**, *35* (6), 442–446.  
537 <https://doi.org/10.1111/phpp.12439>.
- 538 (5) Giokas, D. L.; Salvador, A.; Chisvert, A. UV Filters: From Sunscreens to Human Body and  
539 the Environment. *TrAC Trends in Analytical Chemistry* **2007**, *26* (5), 360–374.  
540 <https://doi.org/10.1016/j.trac.2007.02.012>.
- 541 (6) Damiani, E.; Astolfi, P.; Giesinger, J.; Ehlis, T.; Herzog, B.; Greci, L.; Baschong, W.  
542 Assessment of the Photo-Degradation of UV-Filters and Radical-Induced Peroxidation in  
543 Cosmetic Sunscreen Formulations. *Free Radical Research* **2010**, *44* (3), 304–312.  
544 <https://doi.org/10.3109/10715760903486065>.
- 545 (7) Levine, A. Sunscreen Use and Awareness of Chemical Toxicity among Beach Goers in Hawaii  
546 Prior to a Ban on the Sale of Sunscreens Containing Ingredients Found to Be Toxic to Coral  
547 Reef Ecosystems. *Marine Policy* **2020**, *117*, 103875.  
548 <https://doi.org/10.1016/j.marpol.2020.103875>.
- 549 (8) Downs, C. A.; Kramarsky-Winter, E.; Fauth, J. E.; Segal, R.; Bronstein, O.; Jeger, R.;  
550 Lichtenfeld, Y.; Woodley, C. M.; Pennington, P.; Kushmaro, A.; Loya, Y. Toxicological  
551 Effects of the Sunscreen UV Filter, Benzophenone-2, on Planulae and in Vitro Cells of the  
552 Coral, *Stylophora Pistillata*. *Ecotoxicology* **2014**, *23* (2), 175–191.  
553 <https://doi.org/10.1007/s10646-013-1161-y>.
- 554 (9) Corinaldesi, C.; Marcellini, F.; Nepote, E.; Damiani, E.; Danovaro, R. Impact of Inorganic UV  
555 Filters Contained in Sunscreen Products on Tropical Stony Corals (*Acropora* Spp.). *Science of*  
556 *The Total Environment* **2018**, *637–638*, 1279–1285.  
557 <https://doi.org/10.1016/j.scitotenv.2018.05.108>.
- 558 (10) Ouchene, L.; Litvinov, I. V.; Netchiporouk, E. Hawaii and Other Jurisdictions Ban  
559 Oxybenzone or Octinoxate Sunscreens Based on the Confirmed Adverse Environmental  
560 Effects of Sunscreen Ingredients on Aquatic Environments. *J Cutan Med Surg* **2019**, *23* (6),  
561 648–649. <https://doi.org/10.1177/1203475419871592>.

- 562 (11) Adler, B. L.; DeLeo, V. A. Sunscreen Safety: A Review of Recent Studies on Humans and  
563 the Environment. *Curr Derm Rep* **2020**, *9* (1), 1–9. [https://doi.org/10.1007/s13671-020-](https://doi.org/10.1007/s13671-020-00284-4)  
564 00284-4.
- 565 (12) Widsten, P. Lignin-Based Sunscreens—State-of-the-Art, Prospects and Challenges.  
566 *Cosmetics* **2020**, *7* (4), 85. <https://doi.org/10.3390/cosmetics7040085>.
- 567 (13) Tan, S. S. Y.; MacFarlane, D. R.; Upfal, J.; Edye, L. A.; Doherty, W. O. S.; Patti, A. F.;  
568 Pringle, J. M.; Scott, J. L. Extraction of Lignin from Lignocellulose at Atmospheric Pressure  
569 Using Alkylbenzenesulfonate Ionic Liquid. *Green Chem.* **2009**, *11* (3), 339.  
570 <https://doi.org/10.1039/b815310h>.
- 571 (14) Wei, Z.; Yang, Y.; Yang, R.; Wang, C. Alkaline Lignin Extracted from Furfural Residues  
572 for pH-Responsive Pickering Emulsions and Their Recyclable Polymerization. *Green Chem.*  
573 **2012**, *14* (11), 3230. <https://doi.org/10.1039/c2gc36278c>.
- 574 (15) Thakur, V. K.; Thakur, M. K.; Raghavan, P.; Kessler, M. R. Progress in Green Polymer  
575 Composites from Lignin for Multifunctional Applications: A Review. *ACS Sustainable Chem.*  
576 *Eng.* **2014**, *2* (5), 1072–1092. <https://doi.org/10.1021/sc500087z>.
- 577 (16) Ragauskas, A. J.; Beckham, G. T.; Bidy, M. J.; Chandra, R.; Chen, F.; Davis, M. F.;  
578 Davison, B. H.; Dixon, R. A.; Gilna, P.; Keller, M.; Langan, P.; Naskar, A. K.; Saddler, J. N.;  
579 Tschaplinski, T. J.; Tuskan, G. A.; Wyman, C. E. Lignin Valorization: Improving Lignin  
580 Processing in the Biorefinery. *Science* **2014**, *344* (6185), 1246843.  
581 <https://doi.org/10.1126/science.1246843>.
- 582 (17) Calvo-Flores, F. G.; Dobado, J. A. Lignin as Renewable Raw Material. *ChemSusChem*  
583 **2010**, *3* (11), 1227–1235.
- 584 (18) Bajwa, D. S.; Pourhashem, G.; Ullah, A. H.; Bajwa, S. G. A Concise Review of Current  
585 Lignin Production, Applications, Products and Their Environmental Impact. *Industrial Crops*  
586 *and Products* **2019**, *139*, 111526. <https://doi.org/10.1016/j.indcrop.2019.111526>.
- 587 (19) Qian, Y.; Qiu, X.; Zhu, S. Lignin: A Nature-Inspired Sun Blocker for Broad-Spectrum  
588 Sunscreens. *Green Chem.* **2015**, *17* (1), 320–324. <https://doi.org/10.1039/C4GC01333F>.
- 589 (20) Qian, Y.; Qiu, X.; Zhu, S. Sunscreen Performance of Lignin from Different Technical  
590 Resources and Their General Synergistic Effect with Synthetic Sunscreens. *ACS Sustainable*  
591 *Chem. Eng.* **2016**, *4* (7), 4029–4035. <https://doi.org/10.1021/acssuschemeng.6b00934>.
- 592 (21) Wang, J.; Deng, Y.; Qian, Y.; Qiu, X.; Ren, Y.; Yang, D. Reduction of Lignin Color via  
593 One-Step UV Irradiation. *Green Chem.* **2016**, *18* (3), 695–699.  
594 <https://doi.org/10.1039/C5GC02180D>.
- 595 (22) Qian, Y.; Zhong, X.; Li, Y.; Qiu, X. Fabrication of Uniform Lignin Colloidal Spheres for  
596 Developing Natural Broad-Spectrum Sunscreens with High Sun Protection Factor. *Industrial*  
597 *Crops and Products* **2017**, *101*, 54–60. <https://doi.org/10.1016/j.indcrop.2017.03.001>.
- 598 (23) Gordobil, O.; Herrera, R.; Yahyaoui, M.; İlk, S.; Kaya, M.; Labidi, J. Potential Use of Kraft  
599 and Organosolv Lignins as a Natural Additive for Healthcare Products. *RSC Adv.* **2018**, *8* (43),  
600 24525–24533. <https://doi.org/10.1039/C8RA02255K>.
- 601 (24) Lee, S. C.; Tran, T. M. T.; Choi, J. W.; Won, K. Lignin for White Natural Sunscreens.  
602 *International Journal of Biological Macromolecules* **2019**, *122*, 549–554.  
603 <https://doi.org/10.1016/j.ijbiomac.2018.10.184>.
- 604 (25) Lee, S. C.; Yoo, E.; Lee, S. H.; Won, K. Preparation and Application of Light-Colored  
605 Lignin Nanoparticles for Broad-Spectrum Sunscreens. *Polymers* **2020**, *12* (3), 699.  
606 <https://doi.org/10.3390/polym12030699>.

- 607 (26) Wang, B.; Sun, D.; Wang, H.-M.; Yuan, T.-Q.; Sun, R.-C. Green and Facile Preparation of  
608 Regular Lignin Nanoparticles with High Yield and Their Natural Broad-Spectrum Sunscreens.  
609 *ACS Sustainable Chem. Eng.* **2019**, *7* (2), 2658–2666.  
610 <https://doi.org/10.1021/acssuschemeng.8b05735>.
- 611 (27) Zhang, H.; Liu, X.; Fu, S.; Chen, Y. Fabrication of Light-Colored Lignin Microspheres for  
612 Developing Natural Sunscreens with Favorable UV Absorbability and Staining Resistance.  
613 *Ind. Eng. Chem. Res.* **2019**, *58* (31), 13858–13867. <https://doi.org/10.1021/acs.iecr.9b02086>.
- 614 (28) Zhang, H.; Liu, X.; Fu, S.; Chen, Y. High-Value Utilization of Kraft Lignin: Color  
615 Reduction and Evaluation as Sunscreen Ingredient. *International Journal of Biological*  
616 *Macromolecules* **2019**, *133*, 86–92. <https://doi.org/10.1016/j.ijbiomac.2019.04.092>.
- 617 (29) Trevisan, H.; Rezende, C. A. Pure, Stable and Highly Antioxidant Lignin Nanoparticles  
618 from Elephant Grass. *Industrial Crops and Products* **2020**, *145*, 112105.  
619 <https://doi.org/10.1016/j.indcrop.2020.112105>.
- 620 (30) Ratanasumarn, N.; Chitprasert, P. Cosmetic Potential of Lignin Extracts from Alkaline-  
621 Treated Sugarcane Bagasse: Optimization of Extraction Conditions Using Response Surface  
622 Methodology. *International Journal of Biological Macromolecules* **2020**, *153*, 138–145.  
623 <https://doi.org/10.1016/j.ijbiomac.2020.02.328>.
- 624 (31) Widsten, P.; Tamminen, T.; Liittä, T. Natural Sunscreens Based on Nanoparticles of  
625 Modified Kraft Lignin (CatLignin). *ACS Omega* **2020**, *5* (22), 13438–13446.  
626 <https://doi.org/10.1021/acsomega.0c01742>.
- 627 (32) Ugartondo, V.; Mitjans, M.; Vinardell, M. Comparative Antioxidant and Cytotoxic Effects  
628 of Lignins from Different Sources. *Bioresource Technology* **2008**, *99* (14), 6683–6687.  
629 <https://doi.org/10.1016/j.biortech.2007.11.038>.
- 630 (33) Tortora, M.; Cavalieri, F.; Mosesso, P.; Ciaffardini, F.; Melone, F.; Crestini, C. Ultrasound  
631 Driven Assembly of Lignin into Microcapsules for Storage and Delivery of Hydrophobic  
632 Molecules. *Biomacromolecules* **2014**, *15* (5), 1634–1643. <https://doi.org/10.1021/bm500015j>.
- 633 (34) Gil-Chávez, G. J.; Padhi, S. S. P.; Pereira, C. V.; Guerreiro, J. N.; Matias, A. A.; Smirnova,  
634 I. Cytotoxicity and Biological Capacity of Sulfur-Free Lignins Obtained in Novel Biorefining  
635 Process. *International Journal of Biological Macromolecules* **2019**, *136*, 697–703.  
636 <https://doi.org/10.1016/j.ijbiomac.2019.06.021>.
- 637 (35) Gordobil, O.; Oberemko, A.; Saulis, G.; Baublys, V.; Labidi, J. In Vitro Cytotoxicity  
638 Studies of Industrial Eucalyptus Kraft Lignins on Mouse Hepatoma, Melanoma and Chinese  
639 Hamster Ovary Cells. *International Journal of Biological Macromolecules* **2019**, *135*, 353–  
640 361. <https://doi.org/10.1016/j.ijbiomac.2019.05.111>.
- 641 (36) Freitas, F. M. C.; Cerqueira, M. A.; Gonçalves, C.; Azinheiro, S.; Garrido-Maestu, A.;  
642 Vicente, A. A.; Pastrana, L. M.; Teixeira, J. A.; Michelin, M. Green Synthesis of Lignin Nano-  
643 and Micro-Particles: Physicochemical Characterization, Bioactive Properties and Cytotoxicity  
644 Assessment. *International Journal of Biological Macromolecules* **2020**, *163*, 1798–1809.  
645 <https://doi.org/10.1016/j.ijbiomac.2020.09.110>.
- 646 (37) Menima-Medzogo, J. A.; Walz, K.; Lauer, J. C.; Sivasankarapillai, G.; Gleuwitz, F. R.;  
647 Rolaufts, B.; Laborie, M.-P.; Hart, M. L. Characterization and In Vitro Cytotoxicity Safety  
648 Screening of Fractionated Organosolv Lignin on Diverse Primary Human Cell Types  
649 Commonly Used in Tissue Engineering. *Biology* **2022**, *11* (5), 696.  
650 <https://doi.org/10.3390/biology11050696>.
- 651 (38) Ralph, J.; Lundquist, K.; Brunow, G.; Lu, F.; Kim, H.; Schatz, P. F.; Marita, J. M.; Hatfield,  
652 R. D.; Ralph, S. A.; Christensen, J. H.; Boerjan, W. Lignins: Natural Polymers from Oxidative

- 653 Coupling of 4-Hydroxyphenyl- Propanoids. *Phytochemistry Reviews* **2004**, 3 (1–2), 29–60.  
654 <https://doi.org/10.1023/B:PHYT.0000047809.65444.a4>.
- 655 (39) Akinosho, H. O.; Yoo, C. G.; Dumitrache, A.; Natzke, J.; Muchero, W.; Brown, S. D.;  
656 Ragauskas, A. J. Elucidating the Structural Changes to *Populus* Lignin during Consolidated  
657 Bioprocessing with *Clostridium Thermocellum*. *ACS Sustainable Chem. Eng.* **2017**, 5 (9),  
658 7486–7491. <https://doi.org/10.1021/acssuschemeng.7b01203>.
- 659 (40) *Lignin Structure and Reactions*; Marton, J., Ed.; Advances in Chemistry; AMERICAN  
660 CHEMICAL SOCIETY: WASHINGTON, D.C., 1966; Vol. 59. [https://doi.org/10.1021/ba-](https://doi.org/10.1021/ba-1966-0059)  
661 1966-0059.
- 662 (41) Lanzalunga, O.; Bietti, M. Photo- and Radiation Chemical Induced Degradation of Lignin  
663 Model Compounds. *Journal of Photochemistry and Photobiology B: Biology* **2000**, 56 (2–3),  
664 85–108. [https://doi.org/10.1016/S1011-1344\(00\)00054-3](https://doi.org/10.1016/S1011-1344(00)00054-3).
- 665 (42) Barsberg, S.; Elder, T.; Felby, C. Lignin–Quinone Interactions: Implications for Optical  
666 Properties of Lignin. *Chem. Mater.* **2003**, 15 (3), 649–655.  
667 <https://doi.org/10.1021/cm021162s>.
- 668 (43) Luo, H.; Abu-Omar, M. M. Chemicals From Lignin. In *Encyclopedia of Sustainable*  
669 *Technologies*; Elsevier, 2017; pp 573–585. [https://doi.org/10.1016/B978-0-12-409548-](https://doi.org/10.1016/B978-0-12-409548-9.10235-0)  
670 9.10235-0.
- 671 (44) Mandlekar, N.; Cayla, A.; Rault, F.; Giraud, S.; Salaün, F.; Malucelli, G.; Guan, J.-P. An  
672 Overview on the Use of Lignin and Its Derivatives in Fire Retardant Polymer Systems. In  
673 *Lignin - Trends and Applications*; Poletto, M., Ed.; InTech, 2018.  
674 <https://doi.org/10.5772/intechopen.72963>.
- 675 (45) Demuner, I. F.; Colodette, J. L.; Demuner, A. J.; Jardim, C. M. Biorefinery Review: Wide-  
676 Reaching Products through Kraft Lignin. *BioRes* **2019**, 14 (3), 7543–7581.  
677 <https://doi.org/10.15376/biores.14.3.Demuner>.
- 678 (46) Strassberger, Z.; Tanase, S.; Rothenberg, G. The Pros and Cons of Lignin Valorisation in  
679 an Integrated Biorefinery. *RSC Adv.* **2014**, 4 (48), 25310–25318.  
680 <https://doi.org/10.1039/C4RA04747H>.
- 681 (47) Vishtal, A.; Kraslawski, A. CHALLENGES IN INDUSTRIAL APPLICATIONS OF  
682 TECHNICAL LIGNINS.
- 683 (48) Eraghi Kazzaz, A.; Fatehi, P. Technical Lignin and Its Potential Modification Routes: A  
684 Mini-Review. *Industrial Crops and Products* **2020**, 154, 112732.  
685 <https://doi.org/10.1016/j.indcrop.2020.112732>.
- 686 (49) Kumari, D.; Singh, R. Pretreatment of Lignocellulosic Wastes for Biofuel Production: A  
687 Critical Review. *Renewable and Sustainable Energy Reviews* **2018**, 90, 877–891.  
688 <https://doi.org/10.1016/j.rser.2018.03.111>.
- 689 (50) Ab Rasid, N. S.; Shamjuddin, A.; Abdul Rahman, A. Z.; Amin, N. A. S. Recent Advances  
690 in Green Pre-Treatment Methods of Lignocellulosic Biomass for Enhanced Biofuel  
691 Production. *Journal of Cleaner Production* **2021**, 321, 129038.  
692 <https://doi.org/10.1016/j.jclepro.2021.129038>.
- 693 (51) Matsakas, L.; Karnaouri, A.; Cwirzen, A.; Rova, U.; Christakopoulos, P. Formation of  
694 Lignin Nanoparticles by Combining Organosolv Pretreatment of Birch Biomass and  
695 Homogenization Processes. *Molecules* **2018**, 23 (7), 1822.  
696 <https://doi.org/10.3390/molecules23071822>.
- 697 (52) Adamczyk, J.; Beisl, S.; Amini, S.; Jung, T.; Zikeli, F.; Labidi, J.; Friedl, A. Production and  
698 Properties of Lignin Nanoparticles from Ethanol Organosolv Liquors—Influence of Origin

- 699 and Pretreatment Conditions. *Polymers* **2021**, *13* (3), 384.  
700 <https://doi.org/10.3390/polym13030384>.
- 701 (53) Raj, S.; Jose, S.; Sumod, U.; Sabitha, M. Nanotechnology in Cosmetics: Opportunities and  
702 Challenges. *J Pharm Bioall Sci* **2012**, *4* (3), 186. <https://doi.org/10.4103/0975-7406.99016>.
- 703 (54) Frangville, C.; Rutkevicius, M.; Richter, A. P.; Velev, O. D.; Stoyanov, S. D.; Paunov, V.  
704 N. Fabrication of Environmentally Biodegradable Lignin Nanoparticles. *ChemPhysChem*  
705 **2012**, *13* (18), 4235–4243. <https://doi.org/10.1002/cphc.201200537>.
- 706 (55) Richter, A. P.; Bharti, B.; Armstrong, H. B.; Brown, J. S.; Plemmons, D.; Paunov, V. N.;  
707 Stoyanov, S. D.; Velev, O. D. Synthesis and Characterization of Biodegradable Lignin  
708 Nanoparticles with Tunable Surface Properties. *Langmuir* **2016**, *32* (25), 6468–6477.  
709 <https://doi.org/10.1021/acs.langmuir.6b01088>.
- 710 (56) Lievonen, M.; Valle-Delgado, J. J.; Mattinen, M.-L.; Hult, E.-L.; Lintinen, K.; Kostainen,  
711 M. A.; Paananen, A.; Szilvay, G. R.; Setälä, H.; Österberg, M. A Simple Process for Lignin  
712 Nanoparticle Preparation. *Green Chem.* **2016**, *18* (5), 1416–1422.  
713 <https://doi.org/10.1039/C5GC01436K>.
- 714 (57) Ju, T.; Zhang, Z.; Li, Y.; Miao, X.; Ji, J. Continuous Production of Lignin Nanoparticles  
715 Using a Microchannel Reactor and Its Application in UV-Shielding Films. *RSC Adv.* **2019**, *9*  
716 (43), 24915–24921. <https://doi.org/10.1039/C9RA05064G>.
- 717 (58) Conner, C. G.; Veleva, A. N.; Paunov, V. N.; Stoyanov, S. D.; Velev, O. D. Scalable  
718 Formation of Concentrated Monodisperse Lignin Nanoparticles by Recirculation-Enhanced  
719 Flash Nanoprecipitation. *Part. Part. Syst. Charact.* **2020**, *37* (7), 2000122.  
720 <https://doi.org/10.1002/ppsc.202000122>.
- 721 (59) Ma, M.; Dai, L.; Xu, J.; Liu, Z.; Ni, Y. A Simple and Effective Approach to Fabricate  
722 Lignin Nanoparticles with Tunable Sizes Based on Lignin Fractionation. *Green chemistry : an*  
723 *international journal and green chemistry resource : GC* **2020**, *22* (6), 211–217.
- 724 (60) Morsali, M.; Moreno, A.; Loukovitou, A.; Pylypchuk, I.; Sipponen, M. H. Stabilized  
725 Lignin Nanoparticles for Versatile Hybrid and Functional Nanomaterials. *Biomacromolecules*  
726 **2022**, *23* (11), 4597–4606. <https://doi.org/10.1021/acs.biomac.2c00840>.
- 727 (61) Gilca, I. A.; Popa, V. I.; Crestini, C. Obtaining Lignin Nanoparticles by Sonication.  
728 *Ultrasonics Sonochemistry* **2015**, *23*, 369–375.  
729 <https://doi.org/10.1016/j.ultsonch.2014.08.021>.
- 730 (62) Nair, S. S.; Sharma, S.; Pu, Y.; Sun, Q.; Pan, S.; Zhu, J. Y.; Deng, Y.; Ragauskas, A. J.  
731 High Shear Homogenization of Lignin to Nanolignin and Thermal Stability of Nanolignin-  
732 Polyvinyl Alcohol Blends. *ChemSusChem* **2014**, *7* (12), 3513–3520.  
733 <https://doi.org/10.1002/cssc.201402314>.
- 734 (63) Juikar, S. J.; Vigneshwaran, N. Extraction of Nanolignin from Coconut Fibers by  
735 Controlled Microbial Hydrolysis. *Industrial Crops and Products* **2017**, *109*, 420–425.  
736 <https://doi.org/10.1016/j.indcrop.2017.08.067>.
- 737 (64) Garcia Gonzalez, M. N.; Levi, M.; Turri, S.; Griffini, G. Lignin Nanoparticles by  
738 Ultrasonication and Their Incorporation in Waterborne Polymer Nanocomposites: ARTICLE.  
739 *J. Appl. Polym. Sci.* **2017**, *134* (38), 45318. <https://doi.org/10.1002/app.45318>.
- 740 (65) Mili, M.; Hashmi, S. A. R.; Tilwari, A.; Rathore, S. K. S.; Naik, A.; Srivastava, A. K.;  
741 Verma, S. Preparation of Nanolignin Rich Fraction from Bamboo Stem via Green Technology:  
742 Assessment of Its Antioxidant, Antibacterial and UV Blocking Properties. *Environmental*  
743 *Technology* **2023**, *44* (3), 416–430. <https://doi.org/10.1080/09593330.2021.1973574>.

- 744 (66) Abbati de Assis, C.; Greca, L. G.; Ago, M.; Balakshin, M. Yu.; Jameel, H.; Gonzalez, R.;  
745 Rojas, O. J. Techno-Economic Assessment, Scalability, and Applications of Aerosol Lignin  
746 Micro- and Nanoparticles. *ACS Sustainable Chem. Eng.* **2018**, *6* (9), 11853–11868.  
747 <https://doi.org/10.1021/acssuschemeng.8b02151>.
- 748 (67) Hussin, M. H.; Appaturi, J. N.; Poh, N. E.; Latif, N. H. A.; Brosse, N.; Ziegler-Devin, I.;  
749 Vahabi, H.; Syamani, F. A.; Fatriasari, W.; Solihat, N. N.; Karimah, A.; Iswanto, A. H.; Sekeri,  
750 S. H.; Ibrahim, M. N. M. A Recent Advancement on Preparation, Characterization and  
751 Application of Nanolignin. *International Journal of Biological Macromolecules* **2022**, *200*,  
752 303–326. <https://doi.org/10.1016/j.ijbiomac.2022.01.007>.
- 753 (68) Tan, S.; Liu, D.; Qian, Y.; Wang, J.; Huang, J.; Yi, C.; Qiu, X.; Qin, Y. Towards Better  
754 UV-Blocking and Antioxidant Performance of Varnish via Additives Based on Lignin and Its  
755 Colloids. *Holzforschung* **2019**, *73* (5), 485–491. <https://doi.org/10.1515/hf-2018-0134>.
- 756 (69) El Hage, R.; Brosse, N.; Chrusciel, L.; Sanchez, C.; Sannigrahi, P.; Ragauskas, A.  
757 Characterization of Milled Wood Lignin and Ethanol Organosolv Lignin from Miscanthus.  
758 *Polymer Degradation and Stability* **2009**, *94* (10), 1632–1638.  
759 <https://doi.org/10.1016/j.polymdegradstab.2009.07.007>.
- 760 (70) Steinmetz, V.; Villain-Gambier, M.; Klem, A.; Gambier, F.; Dumarcay, S.; Trebouet, D.  
761 Unveiling TMP Process Water Potential As an Industrial Sourcing of Valuable Lignin–  
762 Carbohydrate Complexes toward Zero-Waste Biorefineries. *ACS Sustainable Chem. Eng.*  
763 **2019**, *7* (6), 6390–6400. <https://doi.org/10.1021/acssuschemeng.9b00181>.
- 764 (71) He, Q.; Ziegler-Devin, I.; Chrusciel, L.; Obame, S. N.; Hong, L.; Lu, X.; Brosse, N. Lignin-  
765 First Integrated Steam Explosion Process for Green Wood Adhesive Application. *ACS*  
766 *Sustainable Chem. Eng.* **2020**, *8* (13), 5380–5392.  
767 <https://doi.org/10.1021/acssuschemeng.0c01065>.
- 768 (72) Sayre, R. M.; Agin, P. P.; LeVee, G. J.; Marlowe, E. A COMPARISON OF IN VIVO AND  
769 IN VITRO TESTING OF SUNSCREENING FORMULAS. *Photochem Photobiol* **1979**, *29*  
770 (3), 559–566. <https://doi.org/10.1111/j.1751-1097.1979.tb07090.x>.
- 771 (73) Meng, X.; Crestini, C.; Ben, H.; Hao, N.; Pu, Y.; Ragauskas, A. J.; Argyropoulos, D. S.  
772 Determination of Hydroxyl Groups in Biorefinery Resources via Quantitative <sup>31</sup>P NMR  
773 Spectroscopy. *Nat Protoc* **2019**, *14* (9), 2627–2647. [https://doi.org/10.1038/s41596-019-0191-](https://doi.org/10.1038/s41596-019-0191-1)  
774 [1](https://doi.org/10.1038/s41596-019-0191-1).
- 775 (74) Brosse, N.; El Hage, R.; Chaouch, M.; Pétrissans, M.; Dumarcay, S.; Gérardin, P.  
776 Investigation of the Chemical Modifications of Beech Wood Lignin during Heat Treatment.  
777 *Polymer Degradation and Stability* **2010**, *95* (9), 1721–1726.  
778 <https://doi.org/10.1016/j.polymdegradstab.2010.05.018>.
- 779 (75) Crestini, C.; Lange, H.; Sette, M.; Argyropoulos, D. S. On the Structure of Softwood Kraft  
780 Lignin. *Green Chem.* **2017**, *19* (17), 4104–4121. <https://doi.org/10.1039/C7GC01812F>.
- 781 (76) Wang, X.; Guo, Y.; Zhou, J.; Sun, G. Structural Changes of Poplar Wood Lignin after  
782 Supercritical Pretreatment Using Carbon Dioxide and Ethanol–Water as Co-Solvents. *RSC*  
783 *Adv.* **2017**, *7* (14), 8314–8322. <https://doi.org/10.1039/C6RA26122A>.
- 784 (77) Siika-aho, M.; Varhimo, A.; Sirviö, J.; Kruus, S. *Sugars from Biomass – High Cellulose*  
785 *Hydrolysability of Oxygen Alkali Treated Spruce, Beech and Wheat Straw*; 2015; Vol. In  
786 Proceedings of the 6th NordicWood Biorefinery Conference 2015.
- 787 (78) Richter, A. P.; Bharti, B.; Armstrong, H. B.; Brown, J. S.; Plemmons, D.; Paunov, V. N.;  
788 Stoyanov, S. D.; Velev, O. D. Synthesis and Characterization of Biodegradable Lignin

- 789 Nanoparticles with Tunable Surface Properties. *Langmuir* **2016**, *32* (25), 6468–6477.  
790 <https://doi.org/10.1021/acs.langmuir.6b01088>.
- 791 (79) Xiong, F.; Han, Y.; Wang, S.; Li, G.; Qin, T.; Chen, Y.; Chu, F. Preparation and Formation  
792 Mechanism of Size-Controlled Lignin Nanospheres by Self-Assembly. *Industrial Crops and*  
793 *Products* **2017**, *100*, 146–152. <https://doi.org/10.1016/j.indcrop.2017.02.025>.
- 794 (80) Ju, T.; Zhang, Z.; Li, Y.; Miao, X.; Ji, J. Continuous Production of Lignin Nanoparticles  
795 Using a Microchannel Reactor and Its Application in UV-Shielding Films. *RSC Adv.* **2019**, *9*  
796 (43), 24915–24921. <https://doi.org/10.1039/C9RA05064G>.
- 797 (81) Manisekaran, A.; Gryan, P.; Duez, B.; Schmidt, D. F.; Lenoble, D.; Thomann, J.-S.  
798 Solvents Drive Self-Assembly Mechanisms and Inherent Properties of Kraft Lignin  
799 Nanoparticles (<50 Nm). *Journal of Colloid and Interface Science* **2022**, *626*, 178–192.  
800 <https://doi.org/10.1016/j.jcis.2022.06.089>.
- 801 (82) Ma, Y.; Liao, Y.; Jiang, Z.; Sun, Q.; Guo, X.; Zhang, W.; Hu, C.; Luque, R.; Shi, B.; Sels,  
802 B. F. Solvent Effect on the Production of Spherical Lignin Nanoparticles. *Green Chem.* **2023**,  
803 *25* (3), 993–1003. <https://doi.org/10.1039/D2GC04014J>.
- 804 (83) Nair, S. S.; Sharma, S.; Pu, Y.; Sun, Q.; Pan, S.; Zhu, J. Y.; Deng, Y.; Ragauskas, A. J.  
805 High Shear Homogenization of Lignin to Nanolignin and Thermal Stability of Nanolignin-  
806 Polyvinyl Alcohol Blends. *ChemSusChem* **2014**, *7* (12), 3513–3520.  
807 <https://doi.org/10.1002/cssc.201402314>.
- 808 (84) Garcia Gonzalez, M. N.; Levi, M.; Turri, S.; Griffini, G. Lignin Nanoparticles by  
809 Ultrasonication and Their Incorporation in Waterborne Polymer Nanocomposites. *J of Applied*  
810 *Polymer Sci* **2017**, *134* (38), 45318. <https://doi.org/10.1002/app.45318>.
- 811 (85) Juikar, S. J.; Vigneshwaran, N. Extraction of Nanolignin from Coconut Fibers by  
812 Controlled Microbial Hydrolysis. *Industrial Crops and Products* **2017**, *109*, 420–425.  
813 <https://doi.org/10.1016/j.indcrop.2017.08.067>.
- 814 (86) Mili, M.; Hashmi, S. A. R.; Tilwari, A.; Rathore, S. K. S.; Naik, A.; Srivastava, A. K.;  
815 Verma, S. Preparation of Nanolignin Rich Fraction from Bamboo Stem via Green Technology:  
816 Assessment of Its Antioxidant, Antibacterial and UV Blocking Properties. *Environmental*  
817 *Technology* **2023**, *44* (3), 416–430. <https://doi.org/10.1080/09593330.2021.1973574>.
- 818 (87) Schneider, W. D. H.; Dillon, A. J. P.; Camassola, M. Lignin Nanoparticles Enter the Scene:  
819 A Promising Versatile Green Tool for Multiple Applications. *Biotechnology Advances* **2021**,  
820 *47*, 107685. <https://doi.org/10.1016/j.biotechadv.2020.107685>.
- 821 (88) Pylypchuk, I. V.; Riazanova, A.; Lindström, M. E.; Sevastyanova, O. Structural and  
822 Molecular-Weight-Dependency in the Formation of Lignin Nanoparticles from Fractionated  
823 Soft- and Hardwood Lignins. *Green Chem.* **2021**, *23* (8), 3061–3072.  
824 <https://doi.org/10.1039/D0GC04058D>.
- 825 (89) Zwilling, J. D.; Jiang, X.; Zambrano, F.; Venditti, R. A.; Jameel, H.; Velev, O. D.; Rojas,  
826 O. J.; Gonzalez, R. Understanding Lignin Micro- and Nanoparticle Nucleation and Growth in  
827 Aqueous Suspensions by Solvent Fractionation. *Green Chem.* **2021**, *23* (2), 1001–1012.  
828 <https://doi.org/10.1039/D0GC03632C>.
- 829 (90) Saad, W. S.; Prud'homme, R. K. Principles of Nanoparticle Formation by Flash  
830 Nanoprecipitation. *Nano Today* **2016**, *11* (2), 212–227.  
831 <https://doi.org/10.1016/j.nantod.2016.04.006>.
- 832 (91) Tao, J.; Chow, S. F.; Zheng, Y. Application of Flash Nanoprecipitation to Fabricate Poorly  
833 Water-Soluble Drug Nanoparticles. *Acta Pharmaceutica Sinica B* **2019**, *9* (1), 4–18.  
834 <https://doi.org/10.1016/j.apsb.2018.11.001>.

- 835 (92) Beisl, S.; Miltner, A.; Friedl, A. Lignin from Micro- to Nanosize: Production Methods.  
836 *IJMS* **2017**, *18* (6), 1244. <https://doi.org/10.3390/ijms18061244>.
- 837 (93) Tian, D.; Hu, J.; Chandra, R. P.; Saddler, J. N.; Lu, C. Valorizing Recalcitrant Cellulolytic  
838 Enzyme Lignin via Lignin Nanoparticles Fabrication in an Integrated Biorefinery. *ACS*  
839 *Sustainable Chem. Eng.* **2017**, *5* (3), 2702–2710.  
840 <https://doi.org/10.1021/acssuschemeng.6b03043>.
- 841 (94) Zwillling, J. D.; Jiang, X.; Zambrano, F.; Venditti, R. A.; Jameel, H.; Velev, O. D.; Rojas,  
842 O. J.; Gonzalez, R. Understanding Lignin Micro- and Nanoparticle Nucleation and Growth in  
843 Aqueous Suspensions by Solvent Fractionation. *Green Chem.* **2021**, *23* (2), 1001–1012.  
844 <https://doi.org/10.1039/D0GC03632C>.
- 845 (95) Pylypchuk, I. V.; Riazanova, A.; Lindström, M. E.; Sevastyanova, O. Structural and  
846 Molecular-Weight-Dependency in the Formation of Lignin Nanoparticles from Fractionated  
847 Soft- and Hardwood Lignins. *Green Chem.* **2021**, *23* (8), 3061–3072.  
848 <https://doi.org/10.1039/D0GC04058D>.
- 849 (96) Zhang, J.; Tian, Z.; Ji, X.-X.; Zhang, F. Light-Colored Lignin Extraction by Ultrafiltration  
850 Membrane Fractionation for Lignin Nanoparticles Preparation as UV-Blocking Sunscreen.  
851 *International Journal of Biological Macromolecules* **2023**, *231*, 123244.  
852 <https://doi.org/10.1016/j.ijbiomac.2023.123244>.
- 853 (97) Zhang, Y.; Naebe, M. Lignin: A Review on Structure, Properties, and Applications as a  
854 Light-Colored UV Absorber. *ACS Sustainable Chem. Eng.* **2021**, *9* (4), 1427–1442.  
855 <https://doi.org/10.1021/acssuschemeng.0c06998>.
- 856 (98) Widsten, P. Lignin-Based Sunscreens—State-of-the-Art, Prospects and Challenges.  
857 *Cosmetics* **2020**, *7* (4), 85. <https://doi.org/10.3390/cosmetics7040085>.
- 858 (99) Guo; Tian; Shen; Yang; Long; He; Song; Zhang; Zhu; Huang; Deng. Transparent  
859 Cellulose/Technical Lignin Composite Films for Advanced Packaging. *Polymers* **2019**, *11* (9),  
860 1455. <https://doi.org/10.3390/polym11091455>.
- 861 (100) Yearla, S. R.; Padmasree, K. Preparation and Characterisation of Lignin Nanoparticles:  
862 Evaluation of Their Potential as Antioxidants and UV Protectants. *Journal of Experimental*  
863 *Nanoscience* **2016**, *11* (4), 289–302. <https://doi.org/10.1080/17458080.2015.1055842>.
- 864